Chapter 4
Distribution of Air: Ventilation Distribution and Heterogeneity

Gregory King and Sylvia Verbanck

4.1 Ventilatory Dead Space

4.1.1 Definition

Ventilatory dead space is the proportion of ventilation that goes to non-gas-exchanging compartments of the lung. Therefore, dead space occurs anatomically by the absence of alveolar structures in a bronchial/bronchiolar airway wall, i.e., the conducting airways. These conducting airways form the anatomical dead space, which is approximately 150 ml in healthy adults (~ 2 ml/kg). Ventilatory dead space can also be created by functional changes, when pulmonary capillary blood flow ceases to a ventilated part of the lung, i.e., when ventilation is present but no pulmonary perfusion so that the ventilation/perfusion ratio is infinite, i.e., $\dot{V}/\dot{Q} = \infty$ (because $\dot{Q} = 0$). This is thus the physiological dead space and is larger than anatomical dead space.

4.1.2 Measurement

Total ventilation (minute ventilation - $\dot{V}_E$) = alveolar ventilation ($\dot{V}_A$) + dead space ventilation ($\dot{V}_D$). Alveolar ventilation, being the part of ventilation that goes to perfused alveoli, is responsible for the exchange of CO_2. Hence $\dot{V}_D$ is measured by

G. King (✉)
Woolcock Institute of Medical Research, The University of Sydney, Sydney, NSW, Australia
e-mail: gregory.king@sydney.edu.au

S. Verbanck
Respiratory Division, University Hospital, UZ Brussel, Brussels, Belgium
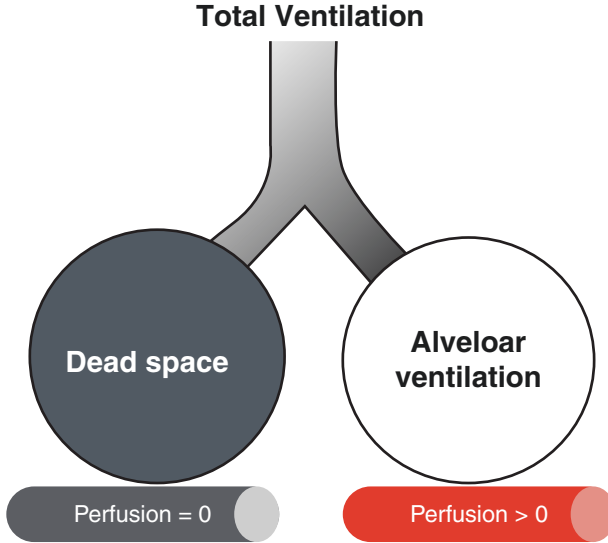e-mail: sylvia.verbanck@uzbrussel.be

Total Ventilation

Fig. 4.1 Alveolar and dead space ventilation are represented by the two compartments. Dead space ventilation, by definition, has no pulmonary perfusion to it; therefore the CO_2 partial pressure is the same as the inspired air. Alveolar ventilation, by definition, has a measurable perfusion; therefore, its CO_2 partial pressure is the same as mixed venous. During exhalation, "dead space" gas and "alveolar ventilation" gas mix together and can be sampled at the mouth (mixed expired gas). If $\dot{V}_A$ and $\dot{V}_D$ are equal, then mixed expired CO_2 would be half that of alveolar CO_2. This proportionality thus allows calculation of $\dot{V}_D$

efficiency of CO_2 clearance from the lungs. If dead space is high, then efficiency becomes low and total ventilation ($\dot{V}_E$) will clear less CO_2 than when efficiency is high (low $\dot{V}_D$). This can be measured by looking at the difference between alveolar CO_2 and "mixed expired CO_2," the latter being a mixture of both alveolar ventilation (high CO_2 content) and dead space ventilation (negligible CO_2 content). Therefore, as dead space ventilation increases, the difference between CO_2 content in alveoli and "mixed expired CO_2" will also proportionally increase (see Fig. 4.1).

Thus $\dot{V}_D$ can be estimated by measuring the difference between alveolar CO_2 (estimated by arterial CO_2), and mixed expired CO_2 as per a simplification of the Bohr equation:

$$\text{Physiological dead space}: \frac{V_D}{V_T} = \frac{\text{PaCO}_2 - P\left(\text{mixed expired CO}_2\right)}{\text{PaCO}_2}$$

The estimation implies that ventilation perfusion mismatch will also increase dead space. That is, in lung units where ventilation is high relative to perfusion (high $\dot{V}/\dot{Q}$), alveolar CO_2 in these units will be low relative to units where $\dot{V}/\dot{Q}$ is ideal, i.e., a ratio around 1. Therefore, ventilation to those units with high $\dot{V}/\dot{Q}$ will contribute to physiological dead space.

4.1.3 Determinants in Health and Disease

Physiological dead space is increased in many common respiratory diseases, particularly obstructive airway diseases and pulmonary vascular diseases. Gas exchange studies using the multiple inert gas elimination test, also known as MIGET studies, show increased ventilatory dead space and high $\dot{V}/\dot{Q}$ in asthma and COPD. The mechanisms presumably include local vascular constriction and destruction due to inflammation and remodeling, with or without secondary pulmonary hypertension. In pulmonary vascular diseases, the decrease in pulmonary vascular blood flow may be heterogeneously distributed, and if ventilation to these units is not reduced to maintain ideal $\dot{V}/\dot{Q}$ by constricting the subtending airways, then physiological dead space will increase.

4.1.4 Clinical Relevance

In obstructive airway diseases, the concept of physiological dead space may be useful for understanding the impact of breathing pattern to gas exchange, particularly in severe disease and acute and severe exacerbations. Low tidal volumes and lung hyperinflation will have profound consequences on alveolar ventilation (hence gas exchange) when dead space is large. Dead space to tidal volume ratios (V_D/V_T) will increase with decreasing tidal volumes (given the fixed volume of the dead space). Hence the goals of treatment are to optimize tidal volumes and respiratory rate and reduce lung hyperinflation (which are all closely related to each other) by pharmacologic and ventilatory support strategies.

4.2 Ventilation Distribution

4.2.1 Definition

Ventilation distribution describes the range of ventilation that occurs within the lung. Ventilation in the lung is not homogenous, even in health. Thus ventilation being uneven throughout the lungs has been described as either "inhomogeneous" or "heterogeneous." The terms are interchangeable but heterogeneity has been the most commonly used term in research publications on ventilation distribution. The distribution of ventilation within the lungs can be characterized in terms of how much of the lung is affected by "low" or "poor" ventilation (functional) and in terms of where in the lungs those poorly ventilating units are located (topographical).

The distribution of ventilation, in a functional sense, can be measured using inert gases, i.e., gases that are not absorbed by the lung. The principle is that when ventilation is uneven or heterogeneous, taking a breath of an inert gas will result in inert

gas concentrations that will differ in different parts of the lung. These can then be measured in situ (by imaging techniques) or at the mouth during the subsequent exhalation (by washout techniques).

The most fundamental way by which inert gas concentrations can differ in different lung units (see definition of lung units below) after inhalation is when there are differences in the volume of alveolar gas in lung units at the start of the breath (initial volume), as well as differences in the volume of inert gas that reaches them. This ratio, i.e., inspired volume/initial volume of lung, is named the "specific ventilation" (SV). Assuming complete dilution of inspired inert gas volume into the gas volume of the lungs, the alveolar concentration of the inert gas can be calculated by the dilution factor, which equals the ratio of inspired volume to inspired volume + initial volume. Hence, alveolar concentration of the inspired inert gas and specific ventilation are directly related (alveolar concentration equals the ratio SV/(SV + 1)). In a hypothetical lung with no ventilation heterogeneity, the specific ventilation in all parts of the lung would then correspond to the subject's pre-inspiratory volume (usually RV or FRC) and the volume of inert gas inhaled; the alveolar concentration (hence SV) would be identical everywhere in the lung. Therefore, according to this simple dilution model, the differences in alveolar concentrations of inert gases between different regions of the lung reflect differences in regional ventilation, and so the distribution of the inert gas (or "marker" gas) is a way to measure ventilation heterogeneity.

Another important concept of gas flow within the lung that is fundamental to understanding the determinants of ventilation distribution is that there is both convective gas flow (gas transport along pressure gradients) and diffusive gas flow (gas transport along concentration gradients). The specific ventilation model implicitly assumes that all lung units are supplied with inspired gas by convective flow and that dilution of inspired with the pre-inspiratory alveolar gas is instantaneous due to rapid diffusive equilibration within each lung unit. Considering that in the human lung, convective gas transport is taken over by diffusive gas transport around branching generation 15, the lung units for which gas concentrations reflect differences in specific ventilation are bigger than the fundamental gas exchanging units of the lung, i.e., the acini, which are about 0.1 cm^3 at FRC. Within these acinar units that are small in volume but large in number, a complex mechanism of interplay between convection and diffusion also generates alveolar concentration differences between intra-acinar air spaces.

Most of the present chapter will be dedicated to the inert gas concentration differences arising from specific ventilation differences between lung units larger than acini.

4.2.2   Determinants in Health

The topographical distribution of the inert gas concentrations can be measured using three-dimensional ventilation imaging techniques, which include single photon emission computed tomography (SPECT), positron emission tomography

(PET), and magnetic resonance imaging with hyperpolarized helium3 (H3 MRI) or Xenon-129. Other imaging techniques measure ventilation distribution in a given plane, such as oxygen-enhanced MRI (called specific ventilation imaging, SVI) using 100% oxygen breathing based on the rate that oxygen fills the alveoli, or electrical impedance tomography (EIT) using changes in electrical impedance at the chest wall surface to infer ventilation distribution within the lung slice circumscribed by the electrode belt. Recently, registration algorithms have been applied to high-resolution CT images obtained at two lung inflations to produce three-dimensional maps of local SV. The above imaging modalities used to quantify ventilation heterogeneity in situ differ widely in terms of spatial resolution, due to limitations imposed by the radiation exposure that is deemed acceptable and by the technology of the radiation detectors themselves.

One of the very first ways in which the distribution of ventilation was measured was by scintigraphy, using small radiation counters placed onto the chest wall to measure the distribution of Xe133, a radioactive isotope of an inert gas. This and subsequent studies in different body postures confirmed the role of gravity in determining the distribution of ventilation in healthy subjects, with ventilation being greatest in the lowest lung units in the line of gravity. In the upright posture, specific ventilation is greatest at the lung base (highest inspired volume relative to initial volume) and decreases in the cranial direction.

The underlying basis of the gravitational gradient of regional ventilation in healthy human lungs is the lungs' elastic properties. The pressure volume curve (Fig. 4.2) should be well known to many. It has a curvilinear shape which describes the increase in lung elastic recoil pressure with increasing lung volume. Above FRC, as lung inflation progresses, elastic recoil also increases, relatively linearly, until at a certain volume above which pressure then increases rapidly for very little change in volume (the "genu" or "knee-bend"). This characteristic shape and pressure-volume behavior of the lung are responsible for the distribution of regional ventilation. Below FRC, the shape of the curve changes again and becomes flatter. This is due to airways being closed near RV. As the lung inflates, the airways open,
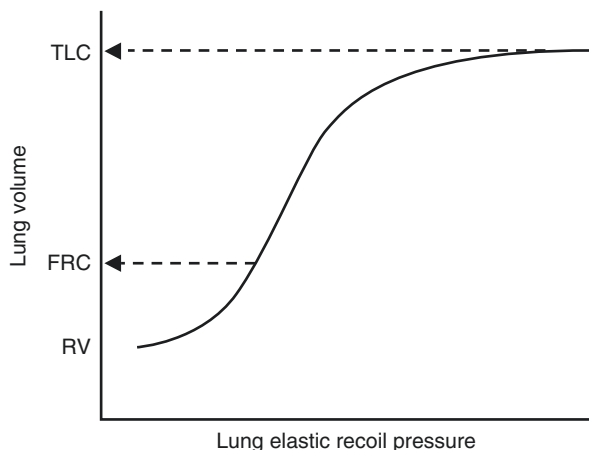

Fig. 4.2 Pressure-volume curve of the lung, measured between RV and TLC. Measurements are usually made using an esophageal balloon, placed near the lung base. However, it is assumed that the pressure-volume characteristics of the lungs are completely uniform

and the slope of the curve increases abruptly with these additional lung units now inflating.

It is assumed that the pressure-volume characteristics of the lung are uniform throughout its entirety. However, the lungs are "suspended" from the top of the chest cavity. At FRC, this then results in the lung tissue being more stretched at the top of the lungs, compared with lower down the lung. Greater distension of the lungs means that lung recoil pressure is greater at the top, i.e., the lung apex operates at a higher portion of the pressure volume curve (as arrowed in Fig. 4.3). Therefore, the top of the lungs is more distended, the alveolar walls are under greater tension, and this region of the lung is operating on the stiffer or "less-compliant" part of the pressure-volume curve. The gradient is approximately 0.2 $cmH_2O/l/s$ per cm of lung height. Therefore, in a lung of 25 cm in height, the transpulmonary pressure may vary from around 8 cmH_2O at the top of the lung to 3 cmH_2O at the bottom.

During a tidal inspiratory breath, the change in pressure across the lung (ΔP in Fig. 4.3) is uniform. The corresponding changes in regional lung volume (ΔV in Fig. 4.3) are greater at the bottom than the top; hence ventilation is greater at the bottom. The greater inert gas concentration in the bottom lung region is thus the combined result of a smaller regional volume at the beginning of inspiration (at FRC) and this region receiving a greater portion of the inhaled volume.
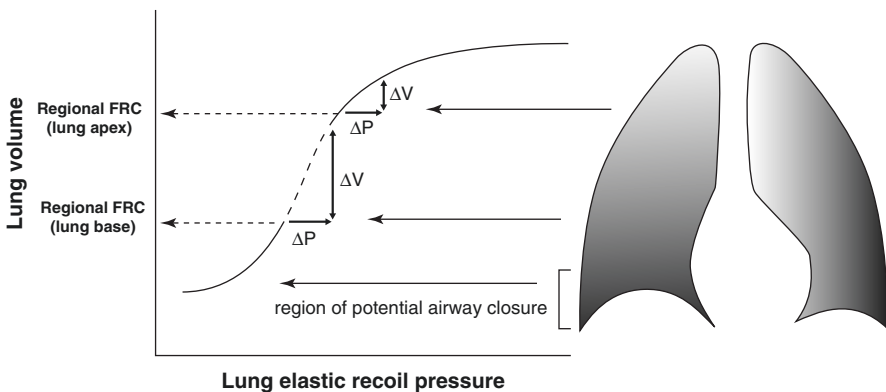

Fig. 4.3 Differences in regional inflation at FRC explain why ventilation differs on a gravitational basis in healthy lungs. The lung apex is subject to greater distending pressure, i.e., on a higher (and stiffer) part of the pressure-volume curve. Therefore, for any given change in pressure (ΔP) during a tidal breath, there is a smaller corresponding change in volume (ΔV or inspired volume) compared with lower in the lung, i.e., the change in lung volume at the base starting from FRC ("regional FRC (lung base)") is greater than the change in lung volume near the apex starting from FRC ("regional FRC (lung apex)"). The shading of the lung diagram demonstrates the gradient of ventilation along the gravitational gradient, during tidal breathing. Darker shading represents greater regional ventilation at the lung bases, and lighter shading represents less regional ventilation further up the lung. At the very base of the lungs, there is a zone where ventilation may be absent, due to airway closure. This zone is only apparent in older age where, during tidal breathing, ventilation to these basal parts of the lung is zero

Airway closure during tidal breathing can be a phenomenon of normal lungs, e.g., normal aging or in obese subjects. Airway closure occurs at the base because lung distending pressure is lowest there, and with decreasing elastic recoil pressure with increasing age, the part of the lung affected by closure increases.

4.2.3 Determinants in Disease

Most is known about changes in ventilation distribution in airway disease, and understanding and measurement of ventilation distribution are probably most relevant in airway diseases. Regional ventilation, i.e., the ventilation in a localized region of the lung, could be altered and differ from that of its neighbor, due to changes in the parenchyma or changes in the airways. In asthma and COPD, there are likely to be changes to both parenchyma and airways.

The inflammatory processes in COPD reduce the lung parenchyma's structure, leading to alveolar enlargement and loss of elastic recoil. There are similar changes in asthma but much subtler than in COPD. There are also changes in airway structure in both asthma and COPD, which alter their function. In asthma, changes in the structure of the airways affect the entire airway wall. Collectively, the changes are referred to as airway remodeling and involve changes to the airway smooth muscle, matrix including the reticular membrane underlying the mucosa which becomes characteristically thickened, mucous glands, and blood vessels. The net result is thickening of the airways and increased airway narrowing and airway closure. In COPD, airway remodeling also occurs, but this is different compared to asthma. There is obliteration of terminal and respiratory bronchioles as well as thinning of the airways walls of small airways.

The combined functional result of pathological changes to the lung parenchyma, its attachment to the airways and to the airways themselves, is airway narrowing and airway closure that is patchy and heterogeneous. Thus, the organization of regional ventilation that is seen in healthy lungs, which is predominantly gravity dependent, is now much more disorganized and "patchy" in distribution. The topographical distribution of ventilation has been well characterized by three-dimensional imaging studies in COPD and in asthma. The images from these studies indicate that there are patchy areas of non-ventilated and poorly-ventilated lung that are apparently randomly located. The pathophysiological basis of this functional abnormality is poorly understood, but functionally, it is likely to be due to the heterogeneous distribution of abnormalities of parenchyma and airways. Although the imaging studies provide a global description of the distribution of ventilation, and show that these regions can be large, subtending from large airways, the determinants of the distribution of ventilation can, in fact, also be large clusters of much smaller airways.

Ventilation in any given region of the lung is determined by the compliance of the lung tissue and resistance of its subtending airways. Multiplying resistance (R) and compliance (C) gives a term known as the time constant (τ), i.e., $\tau = R \times C$, and

its unit is seconds. Those lung units that have long time constants, either from increased *R* or decreased *C* or both, ventilate poorly. Therefore, the increase in ventilation heterogeneity that is typical in asthmatic and COPD lungs can be conceptually described as having an increased range of time constants. This implies that there are some parts of the lungs that ventilate well (short time constants, high flows) and some parts that ventilate poorly (long time constants, low flows). The units might be anatomically co-located, which is what can be observed on ventilation scans, but they can also be scattered around the lungs and may be far apart. This concept that there are poorly ventilating units with long τ is important in understanding how inert gas washout tests are interpreted.

4.2.4   Measurement

Inert gas washout tests were developed 70 years ago with the description of the single-breath nitrogen washout test (SBNW). The SBNW test requires inspiration of 100% oxygen, which dilutes and washes out the nitrogen that is "resident" in the alveoli. Thus, SBNW tests have also been referred to as "resident gas" techniques, which distinguish them from inhaled inert gas tests (wash-in tests), e.g., with argon or helium. To highlight the effect of airway closure, a small bolus of argon or helium gas – instead of a full inspiration – is introduced at the start of the inhalation. The pure oxygen (or inert gases) can be inhaled from any pre-inspiratory volume and the inspired volume can also be varied. The effects of varying pre-inspiratory lung volume and inspired volume provide useful information on the nature of ventilation distribution. In the SBNW, after inhalation of pure oxygen, the subject exhales at a slow even rate, and the concentrations of the expired nitrogen gas are sampled continuously; a typical example of the expired N_2 concentration versus expired volume is in Fig. 4.4.

A useful way to understand the SNBW is by using a two-compartment concept of the lung, putting all the relatively well-ventilated lung units (high SV, short τ) into one functional compartment and the relatively poorly functioning units (low SV, long τ) into another. See Fig. 4.5. This results in two units with two averaged (and different) inert gas concentrations at the end of the inert gas inhalation. During exhalation, the concentrations from these units are then recombined to a concentration in the parent airway (or at the mouth, where the washout gas can be sampled) according to their relative contribution to the expiratory flow (or volume) from each unit. In particular, concentration at the mouth equals (conc1.ΔV1 + conc2.ΔV2)/(ΔV1 + ΔV2). This means that if both units exhale at a different but constant rate ($\dot{V}$ 1 and $\dot{V}$ 2), overall washout concentration will be a ventilation-weighted average of both unit concentrations. Importantly, in that hypothetical case, the washout concentration during the phase III will be constant, resulting in a zero phase III slope. This is because the relative contributions from both compartments at any point in the expiration are constant. However, even in healthy subjects, SBNW
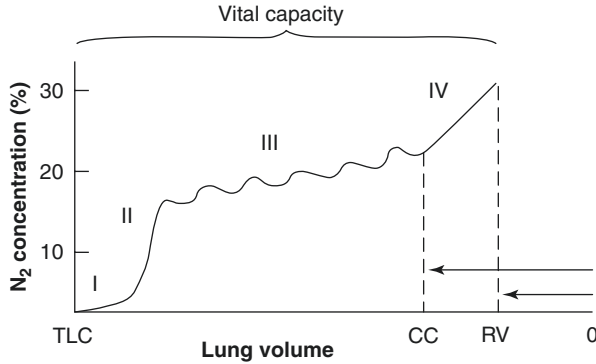
Fig. 4.4 Example of a single-breath nitrogen washout after O_2 inhalation from RV. N_2 nitrogen, CC closing capacity, I phase I, II phase II, III phase III, IV phase IV. The expiration starts from TLC, i.e., exhalation goes from left to right. Phase I gas is pure dead space, i.e., 100% oxygen and therefore 0% nitrogen. The phase II gas is a mix between dead space and alveolar gas. Phase III is alveolar gas and phase IV is gas expired after the onset of airway closure. The arrows indicate the magnitude of the CC and RV. Phase III has bumps to it, which are the cardiogenic oscillations due to heterogeneity of nitrogen concentrations from the heartbeat that intermittently "pushes" gas from higher N_2 regions into the expirate
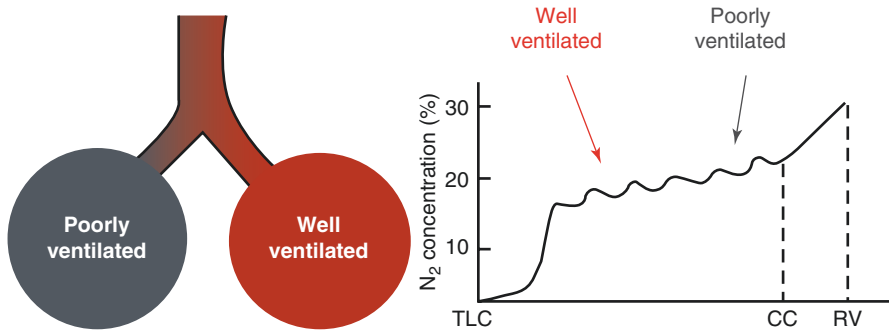

Fig. 4.5 The two-compartment representation of ventilation distribution. Gray indicates slow or poorly ventilating lung units (hence higher N_2 concentrations), and red indicates better or well-ventilated units. The well-ventilated compartment makes a greater contribution to the early part of the phase III (hence lower N_2 concentrations at the start), while the poorly ventilated part contributes more later, explaining the increase in N_2 concentrations as expiration proceeds

phase III slope is always positive, indicating that there must be another mechanism occurring in addition to regional heterogeneity in SV.

The second mechanism that is crucial to understanding the SBNW, and also how ventilation distribution in the lungs translates into a washout curve during exhalation, is that there is sequential emptying of the lung units. That is, not all lung units empty at the same constant rate during the entire exhalation. The best ventilated unit

is said to "empty first," meaning that the unit with the highest flow slows down a little as exhalation continues, in favor of the other slower unit speeding up a little (to maintain the constant expiratory flow rate required in the test). At all times during exhalation, the flow of the best ventilated may well be greatest, but its magnitude relative to the poorly ventilated units must decrease a little in order to explain the positive N_2 slope in the phase III. In Fig. 4.5, the red arrow indicates that the first part of phase III represents alveolar gas from the best ventilated lung units, which have a lower nitrogen concentration due to greater specific ventilation. As exhalation proceeds there is increasing contribution from the poorer ventilated units (gray arrow), which have higher nitrogen concentrations due to their lower specific ventilation. One mechanism of flow sequencing is generated by the effect of gravity, due to the curvilinear shape of the PV curve, and respective contributions to ventilation from upper and lower parts of the lungs as the exhalation progresses from TLC to RV. We also know from SBNW experiments in microgravity that there are also non-gravitational effects generating a phase III slope. In summary, irrespective of the potential mechanisms generating a sequence of lung emptying, it is a necessary condition for the SV differences in the lung to produce a non-zero phase III slope. In this way, the magnitude of the phase III slope is a measure of degree of ventilation heterogeneity.

As exhalation proceeds further and below FRC, airway closure can occur which is characterized by a sudden increase in contribution from poorly ventilated units and hence a sudden increase in nitrogen concentration (phase IV). The point in the exhalation at which phase IV occurs is called the closing point. The absolute lung volume at which closing point occurs is called closing capacity (usually expressed as a percentage of TLC – see Fig. 4.4). The difference between CC and RV is called closing volume (CV – usually expressed as a percentage of VC).

In its original version, in the 1950s, the multiple-breath nitrogen washout (MBNW) was, as the name implies, a concatenation of multiple inhaled breaths of pure oxygen, where the subsequent exhalations were collected and analyzed for expired nitrogen concentration (Fig. 4.6). The plot of concentration versus breath number (or cumulative exhaled volume if available) is usually referred to as the washout (concentration) curve; it is also usually expressed in a semi-log plot since perfect dilution would produce a perfectly linear dependence of log(concentration) versus breath number. Even with an added dead space, the washout concentration curve would still be linear in semi-log plot yet with a slower descent versus a washout with same volumes but no dead space. In the original studies, the number of breaths necessary to reach a certain level of overall nitrogen dilution was translated into an index named the lung clearance index (LCI). In more recent studies, the LCI is derived from the nitrogen and volume trace, measured continuously as a MBNW progresses. The number of lung turnovers (tidal volume over lung volume, VT/FRC) needed to reach 1/40th of the pre-test alveolar concentration equals the LCI. Depending on the study, the concentration used to compute LCI may be mean expired N_2 concentration, average alveolar plateau N_2 concentration or end-tidal N_2 concentration. Depending on this choice, typical values of LCI in the normal lungs will range 5–6. The advantage of LCI is that it is simple to compute and relatively
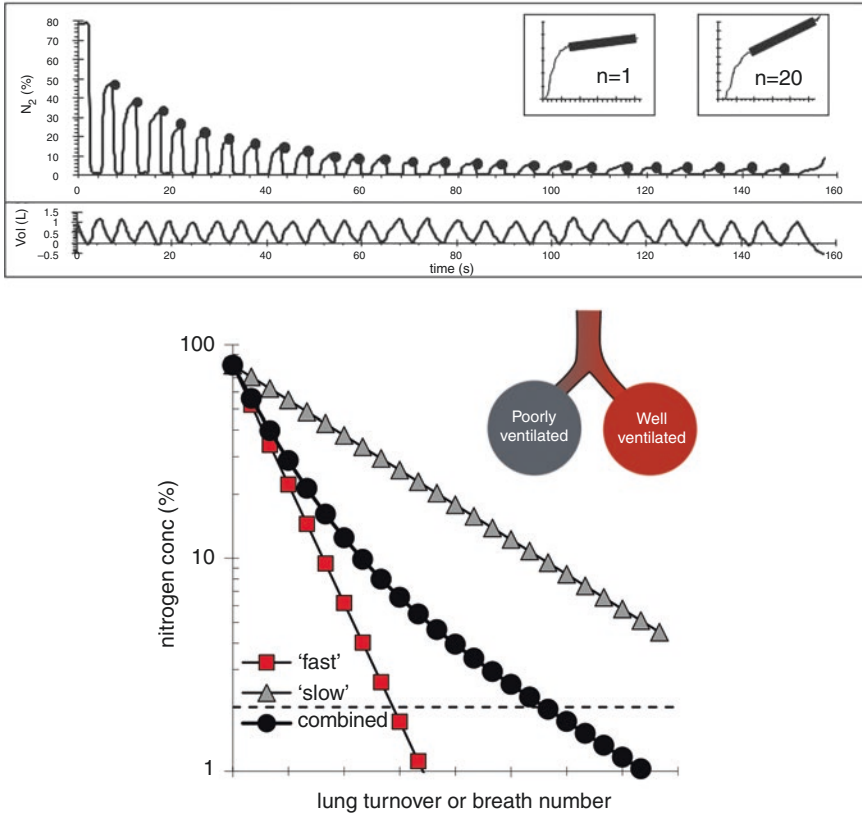
Fig. 4.6 The progressive decrease in nitrogen concentration during a multiple-breath nitrogen washout (MBNW) test (top) and the corresponding semi-log plots of N_2 concentration versus breath number or lung turnover (bottom), conceptually resulting from a combination of a slow and a fast compartment washout curve

independent of the subject's FRC. For example, in a subject with a greater FRC, the unit turnover (VT/FRC in the abscissa) will be smaller, yet the breath-by-breath decrease of N_2 concentration due to dilution is also slower because the same O_2 volume is diluted into a greater FRC. This FRC compensation of dilution, by expressing the concentration washout curve versus lung turnover instead of breath number, is the strength of LCI. The weakness of the LCI is that it is determined in a portion of the washout curve where concentrations are very low and thus prone to measurement error.

Other measures of ventilation heterogeneity have been derived from the MBNW washout concentration curves. Moment ratios are simply computed by considering the concentrations measured in each subsequent breath as a distribution of concentrations from which the various moments (average, standard deviation, skewness) can be computed. There is no information about the spatial distribution of differences in concentrations in the lungs in such analyses. Curvilinearity of the semi-log

plot has also been proposed as a measure of ventilation heterogeneity, where a perfectly linear plot signals a perfectly homogeneously ventilated lung, and the most extreme case of curvilinearity is that where one part of the lungs has an infinitesimally slow time constant τ and therefore an almost horizontal plateau (infinitesimally small decrease in concentration) in the semi-log plot. A real washout concentration plot in health and disease is somewhat curvilinear in a semi-log plot (schematically represented in Fig. 4.6, black dots) and this can be viewed as the lung functioning as two separate compartments, each one washing out at its own pace (according to its own τ) and generating its own (linear) washout curve. An index of curvilinearity is therefore often computed as the relative N_2 concentration decrease in the fast (early) and slow (late) portion of the washout curve measured at the mouth.

In adults, a MBNW maneuver usually consists of repeated inhalations of a fixed volume of pure oxygen (usually 1 liter) from end-expiratory lung volume (usually FRC) at normal breathing flow (typically 10–12 breaths per minute). The repeated inhalation of 1 liter breaths continues until the final nitrogen concentration is near zero (1/40th of the starting concentration). See Fig. 4.6 for an example.

In a more elaborate analysis of MBNW, the entire N_2 concentration and volume trace can be analyzed as if they were a concatenation of individual SBNW curves, where a phase III slope can be computed in each expiratory phase (see Fig. 4.6, top, where a slope for the 1st and the 20th breath is illustrated in the inset). Based on a large body of computational modeling work, it has been suggested that when the phase III slope in each subsequent breath is normalized (divided) by the mean expired concentration (or alveolar concentration), the relative contribution of large-scale ventilation heterogeneities, also visible on imaging, can be distinguished from ventilation heterogeneity occurring beyond the resolution scale of imaging modalities (at acinar level).

The analysis is somewhat complex, but the principal idea of the test is to partition ventilation heterogeneity generated in the convection-dependent airways and ventilation heterogeneity in the respiratory airways beyond those airways where gas also moves by diffusion; the diffusion-dependent airways. The term used to represent ventilation heterogeneity in the convection-dependent airways is Scond. The corresponding term for ventilation heterogeneity in more peripheral and diffusion dependent airways is Sacin. These abbreviations arise from the specific slopes measured ("S"), while "cond" and "acin" refer to conductive and acinar airways, respectively, since these roughly correspond to the air spaces in the lung where convection and diffusion are predominant. In fact, the actual functional boundary between the convection-dependent and the more peripheral diffusion-dependent lung units is the so-called diffusion front, which is a sigmoid-shaped oxygen profile extending between the entrance and the lung periphery. While the diffusion front is not a sharp scission between the conductive and the acinar airways, it is located at the lung depth where the combined lumen cross-sectional areas of the airways increases rapidly (i.e., where alveolation starts), namely where diffusion takes over from convection as the dominant gas transport mechanism.
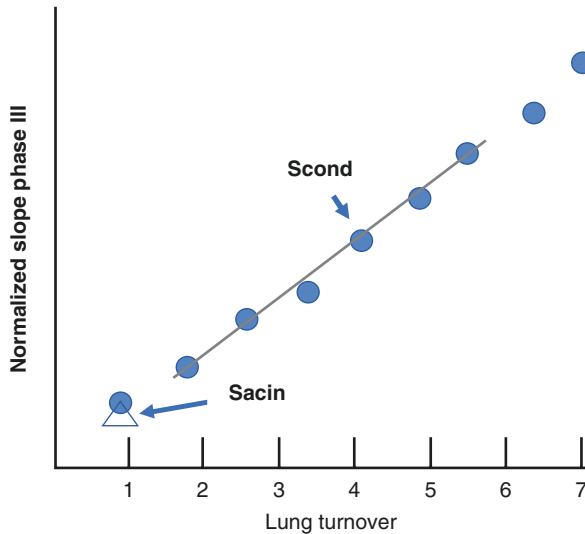
Fig. 4.7 Diagram demonstrating the calculations of Scond and Sacin from the relationship between normalized (for its mean N_2 concentration) Phase III slope of each breath of the washout, plotted against lung turnover (breath volume/FRC). Each blue dot represents each breath during the washout, the number of breaths varying depending on lung size and ventilatory efficiency. The slope of the line fitted to the breaths between turnovers 1.5 and 6 is the value of Scond. The normalized phase III slope of the first breath, with the component of ventilation heterogeneity from Scond subtracted from it (i.e., Scond x lung turnover of the first breath), is the value of Sacin (triangle). Scond and Sacin are calculated from the pooled values of three artifact-free washouts. Therefore, the Sacin calculation will be from the average of three normalized phase III slopes of each of the three washouts and average of their three lung turnovers

The principle of Scond and Sacin computation, both derived from the normalized phase III slope, is as follows (Fig. 4.7). Distribution of oxygen during the first breath of the MBNW is similar to that which occurs in a single-breath washout. The advantage of observing phase III slope in subsequent breaths is that it progressively accentuates concentration differences due to convective gas flow. This principle then allows separation of ventilation heterogeneity due to convection-dependent and diffusion-dependent effects. Ventilation heterogeneity in convection-dependent airways is measured from the rate at which phase III slope increases as the washout progresses. Ventilation heterogeneity in diffusion-dependent airways is measured primarily from the first breath of the washout, since it generates a portion of the phase III that remains almost constant throughout the subsequent breaths; it is calculated as the phase III slope of the first breath from which the calculated (small) contribution of convective ventilation heterogeneity is subtracted. In principle, Scond may represent ventilation heterogeneity in both the large and small conductive airways. Recent four-dimensional CT data in normal man have shown that Scond may be generated between the five lung lobes, whereas during induced bronchoconstriction or in disease, Scond more likely represents ventilation heterogeneity generated between smaller conductive airways.

4.2.5 Clinical Relevance

The phase III slope and CC from SBNW were initially thought to be sensitive indicators of early small airway disease and therefore applied to smokers. However, it appears to be overly sensitive in that at least half of smokers will have an abnormal SBNW index, which suggests that it would not have sufficient specificity to indicate risk of COPD in smokers. In asthma, high phase III slopes and high closing capacity indicate increased risk of severe attacks.

Thus far the lung clearance index derived from the MBNW concentration curve has proven to be clinically useful mostly in cystic fibrosis lung disease, where considerable portions of the lung wash out at a very slow pace. In fact, in adult CF patients, their LCI can be directly linked to the number of bronchial segments affected by bronchiectasis, which slows the ventilation into those parts of the lung. In asthma and COPD, LCI are also elevated but more mildly so than in CF patients for a similar degree of obstruction in terms of spirometry.

Indices from the phase III slope analysis of the MBNW yield insight into the approximate anatomic location of ventilation heterogeneity in the lung, which may be altered by disease (Fig. 4.8).

Scond and Sacin have been shown to correlate strongly with several clinical features of asthma. Scond relates strongly to airway hyperresponsiveness independently of airway inflammation, in subjects under the age of around 50 years. However, in older subjects, Sacin correlates with airway hyperresponsiveness. The
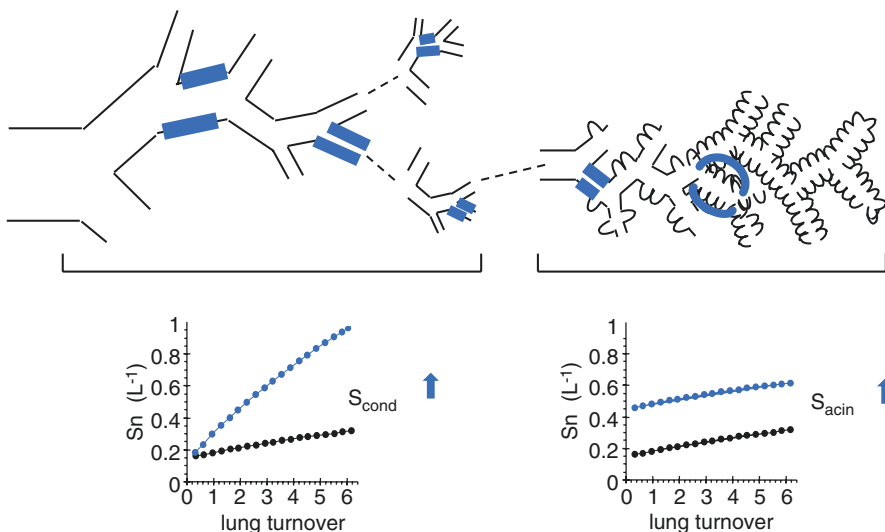

Fig. 4.8 Schematic diagram illustrating how Scond and Sacin are affected by disease. The rate of rise and the offset of the Sn (normalised phase III slope) curves roughly correspond to respectively Scond and Sacin. Scond will typically be affected by structural heterogeneity in the large or conductive small airways. Sacin will typically be affected by structural heterogeneity in the acinar airways

difference was attributed to the age-related changes in lung structure, perhaps with an increasingly important role of the diffusion-dependent airways in older subjects. Interestingly, Scond was also found to predict the magnitude of airway closure that could be induced by methacholine challenge, while Sacin predicted the development of airway narrowing. Both Scond and Sacin relate to symptomatic measures of asthma control, while Sacin predicts the worsening of asthma control when inhaled corticosteroid is reduced in stable asthmatic subjects.

In COPD and smokers, both Sacin and Scond appear to be highly sensitive measures of small airway dysfunction given that they improve following smoking cessation. In smokers with normal spirometry, Sacin relates to smoking history, while Scond relates to bronchitic symptoms. In smokers with overt COPD, where a large number of terminal bronchioles are simply obliterated, Sacin is the most sensitive index to pick up this morphometrical feature. Although the SBNW test has not proven to be clinically useful over time, the MBNW test provides more detailed information and has been shown to have significant clinical correlates in asthma and COPD. The MBNW test is likely to be used in routine clinical practice in the future, although this will be dependent on completion of further informative clinical studies.

Selected References

Bourdin A, Paganin F, Préfaut C, Kieseler D, Godard P, Chanez P. Nitrogen washout slope in poorly controlled asthma. Allergy. 2006;61(1):85–9.

Buist AS, Ross BB. Predicted values for closing volume using a modified single breath nitrogen test. Am Rev Respir Dis. 1973a;107:744–52.

Buist AS, Ross BB. Quantitative analysis of the alveolar plateau in the diagnosis of early airway obstruction. Am Rev Respir Dis. 1973b;108(5):1078–87.

Buist AS, Ghezzo H, Anthonisen NR, Cherniack RM, Ducic S, Macklem PT, Manfreda J, Martin RR, McCarthy D, Ross BB. Relationship between the single-breath N test and age, sex, and smoking habit in three North American cities. Am Rev Respir Dis. 1979;120(2):305–18.

Downie S, Salome C, Verbanck S, Thompson B, Berend N, King G. Ventilation heterogeneity is a major determinant of airway hyperresponsiveness in asthma, independent of airway inflammation. Thorax. 2007;62(8):684–9.

Farah CS, King GG, Brown NJ, Downie SR, Kermode J, Hardaker KM, Peters MJ, Berend N, Salome CM. The role of the small airways in the clinical expression of asthma in adults. J Allergy Clin Immunol. 2012a;129(2):381–7.

Farah CS, King GG, Brown NJ, Peters MJ, Berend N, Salome CM. Ventilation heterogeneity predicts asthma control in adults following inhaled corticosteroid dose titration. J Allergy Clin Immunol. 2012b;130(1):61–8.

Farrow CE, Salome CM, Harris BE, Bailey DL, Bailey E, Berend N, Young IH, King GG. Airway closure on imaging relates to airway hyperresponsiveness and peripheral airway disease in asthma. J Appl Physiol. 2012;113(6):958–66.

Farrow CE, Salome CM, Harris BE, Bailey DL, Berend N, King G. Peripheral ventilation heterogeneity determines the extent of bronchoconstriction in asthma. J Appl Physiol. 2017;123(5):1188–94.

Fowler WS. Lung function studies: II. The respiratory dead space. Am J Phys. 1948;154(3):405–16.

Fowler WS. Lung function studies: III. Uneven pulmonary ventilation in normal subjects and in patients with pulmonary disease. J Appl Physiol. 1949;2:283.

Hardaker KM, Downie SR, Kermode JA, Farah CS, Brown NJ, Berend N, King GG, Salome CM. The predictors of airway hyperresponsiveness differ between old and young asthmatics. Chest. 2011;139(6):1395–401.

Harris RS, Winkler T, Tgavalekos N, Musch G, Melo MFV, Schroeder T, Chang Y, Venegas JG. Regional pulmonary perfusion, inflation, and ventilation defects in bronchoconstricted patients with asthma. Am J Respir Crit Care Med. 2006;174(3):245–53.

In 't Veen JC, Beekman AJ, Bel EH, Sterk PJ. Recurrent exacerbations in severe asthma are associated with enhanced airway closure during stable episodes. Am J Respir Crit Care Med. 2000;161(6):1902–6.

Jetmalani K, Thamrin C, Farah CS, Bertolin A, Berend N, Salome CM, King GG. Peripheral airway dysfunction and relationship with symptoms in smokers with preserved spirometry. Respirology. 2018;23(5):512–8.

King GG, Eberl S, Salome CM, Meikle SR, Woolcock AJ. Airway closure measured by a Technegas bolus and SPECT. Am J Respir Crit Care Med. 1997;155(2):682–8.

King GG, James A, Wark P. The pathophysiology of severe asthma: we've only just started. Respirology. 2018;23(3):262–71.

Mathew L, Kirby M, Etemad-Rezai R, Wheatley A, McCormack D, Parraga G. Hyperpolarized (3) He magnetic resonance imaging: preliminary evaluation of phenotyping potential in chronic obstructive pulmonary disease. Eur J Radiol. 2011;79(1):140–6.

McDonough JE, Yuan R, Suzuki M, Seyednejad N, Elliott WM, Sanchez PG, Wright AC, Gefter WB, Litzky L, Coxson HO, Paré PD, Sin DD, Pierce RA, Woods JC, McWilliams AM, Mayo JR, Lam SC, Cooper JD, Hogg JC. Small-airway obstruction and emphysema in chronic obstructive pulmonary disease. N Engl J Med. 2011;365(17):1567–75.

Milic-Emili J, Henderson JAM, Dolovich MB, Trop D, Kaneko K. Regional distribution of inspired gas in the lung. J Appl Physiol. 1966;21:749–59.

Milic-Emili J, Torchio R, D'Angelo E. Closing volume: a reappraisal (1967–2007). Eur J Appl Physiol. 2007;99(6):567–83.

Tanabe N, Vasilescu DM, McDonough JE, Kinose D, Suzuki M, Cooper JD, Paré PD, Hogg JC. MicroCT comparison of preterminal bronchioles in centrilobular and panlobular emphysema. Am J Respir Crit Care Med. 2017;195(5):630–8.

Thurlbeck WM, Dunnill MS, Hartung W, Heard BE, Heppleston AG, Ryder RC. A comparison of three methods of measuring emphysema. Hum Pathol. 1970;1(2):215–26.

Tzeng Y-S, Lutchen K, Albert M. The difference in ventilation heterogeneity between asthmatic and healthy subjects quantified using hyperpolarized 3He MRI. J Appl Physiol. 2009;106(3):813–22.

Verbanck S, Paiva M. Gas mixing in the airways and airspaces. Compr Physiol. 2011;1:809–34.

Verbanck S, Schuermans D, Van Muylem A, Melot C, Noppen M, Vincken W, Paiva M. Conductive and acinar lung-zone contributions to ventilation inhomogeneity in COPD. Am J Respir Crit Care Med. 1998;157(5 Pt 1):1573–7.

Verbanck S, Schuermans D, Paiva M, Meysman M, Vincken W. Small airway function improvement after smoking cessation in smokers without airway obstruction. Am J Respir Crit Care Med. 2006;174(8):853–7.

Verbanck S, Van Muylem A, Schuermans D, Bautmans I, Thompson B, Vincken W. Transfer factor, lung volumes, resistance and ventilation distribution in healthy adults. Eur Respir J. 2016;47:166–76.

Verbanck S, King GG, Zhou W, Miller A, Thamrin C, Schuermans D, Ilsen B, Ernst CW, de Mey J, Vincken W, Vanderhelst E. The quantitative link of lung clearance index to bronchial segments affected by bronchiectasis. Thorax. 2018a;73(1):82–4.

Verbanck S, King GG, Paiva M, Schuermans D, Vanderhelst E. The functional correlate of the loss of terminal bronchioles in COPD. Am J Respir Crit Care Med. 2018b. https://doi.org/10.1164/rccm.201712-2366LE.